

Impact of noise on inverse design: The case of NMR spectra matching

Supplementary Information

Dominik Lemm^{1,2}, Guido Falk von Rudorff^{3,4} and O. Anatole von Lilienfeld^{5,6,7}

¹ *University of Vienna, Faculty of Physics, Kolingasse 14-16, AT-1090 Vienna, Austria*

² *University of Vienna, Vienna Doctoral School in Physics, Boltzmannngasse 5, AT-1090 Vienna, Austria*

³ *University Kassel, Department of Chemistry, Heinrich-Plett-Str.40, 34132 Kassel, Germany*

⁴ *Center for Interdisciplinary Nanostructure Science and Technology (CINSA-T), Heinrich-Plett-Straße 40, 34132 Kassel*

⁵ *Departments of Chemistry, Materials Science and Engineering, and Physics, University of Toronto, St. George Campus, Toronto, ON, Canada*

⁶ *Vector Institute for Artificial Intelligence, Toronto, ON, M5S 1M1, Canada*

⁷ *Machine Learning Group, Technische Universität Berlin and Institute for the Foundations of Learning and Data, 10587 Berlin, Germany*

*Electronic address: anatole.vonlilienfeld@utoronto.ca

(Dated: 20 September 2023)

TABLE S1. Functional groups contained in the C₇O₂H₁₀ constitutional isomer chemical space and corresponding SMARTS patterns.

Functional Group	SMARTS Pattern
alkene	[CX3]=[CX3]
alkyne	[CX2]#[CX2]
arene	[cX3]1[cX3][cX3][cX3][cX3][cX3]1
alcohol	[#6][OX2H]
aldehyde	CX3H1[#6,H]
ketone	[#6]CX3[#6]
carboxylic acid	CX3[OX2H]
acid anhydride	CX3[OX2]CX3
ester	[#6]CX3[OX2H0][#6]
ether	OD2[#6]
enol	[OX2H][#6X3]=[#6]
phenol	[OX2H][cX3]:[c]

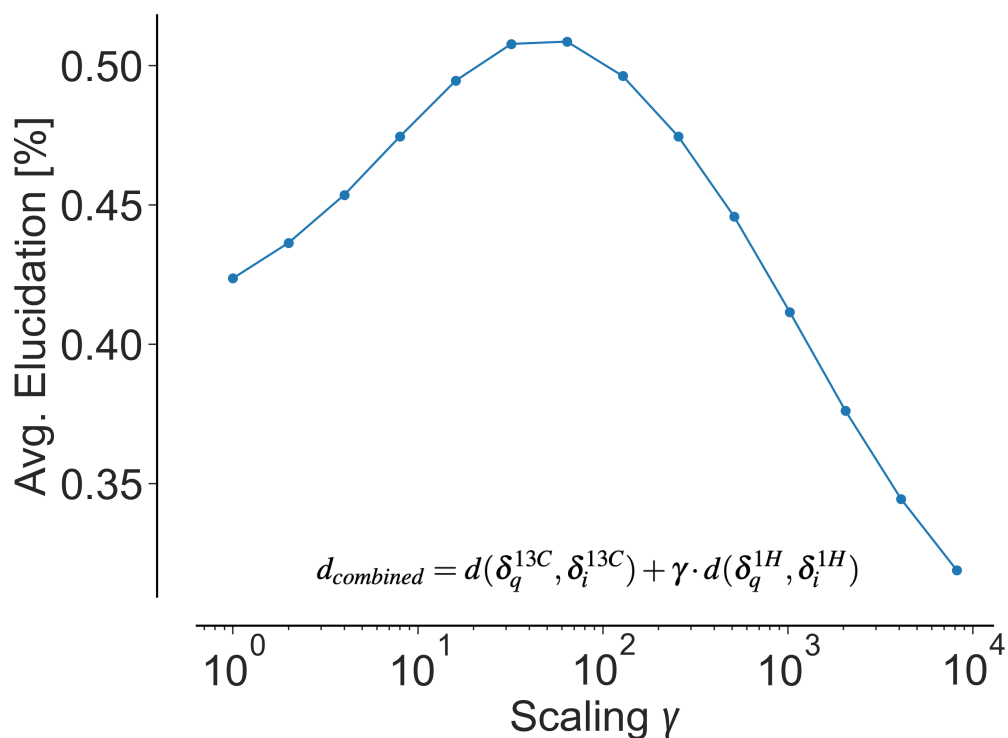


FIG. S1. Hyperparameter scan of γ on C₇O₂H₁₀ constitutional isomers for the combined ranking of ¹³C and ¹H shifts. First, the respective distances of ¹³C and ¹H at their individual shift accuracy levels are being calculated and then the distances combined via the depicted Eq.2. The average elucidation is calculated by averaging across all shift accuracy levels.

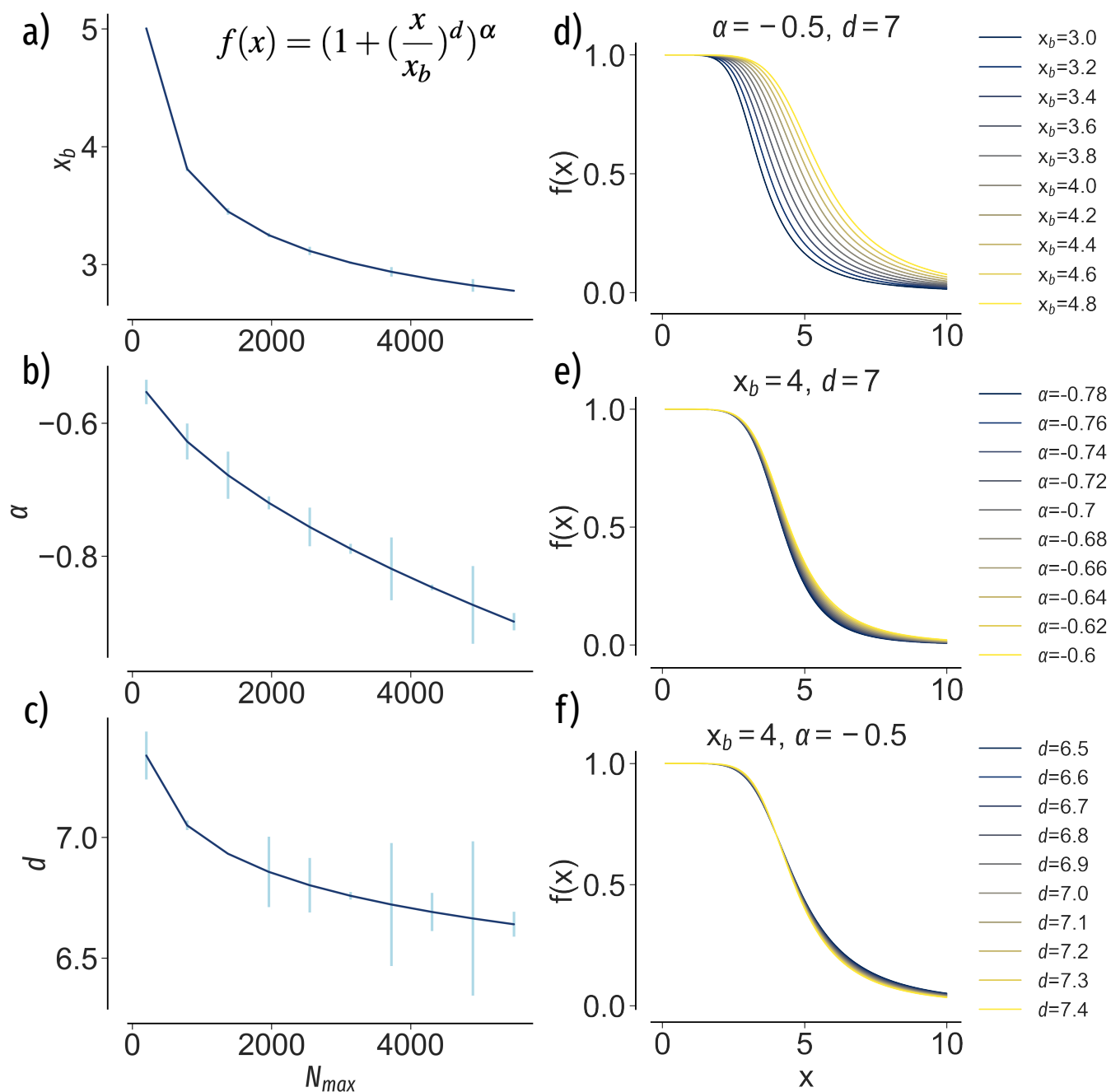


FIG. S2. Parameter distributions of a broken powerlaw function (Eq.3) used for extrapolating the elucidation trends. a-c) Parameters x_b , α and d fitted to the elucidation trends of $C_7O_2H_{10}$ at multiple N_{max} . Note that the parameters d and α are more noisy in nature given the finite sampling and only marginally influence the shape of the curve in the observed parameter range (see e) and f)). Conversely, the parameter x_b , which dictates the offset of the curve, is well behaved and decays smoothly as N_{max} increases. d-f) Influence of the observed parameter ranges for x_b , α and d on the shape of the broken powerlaw function.

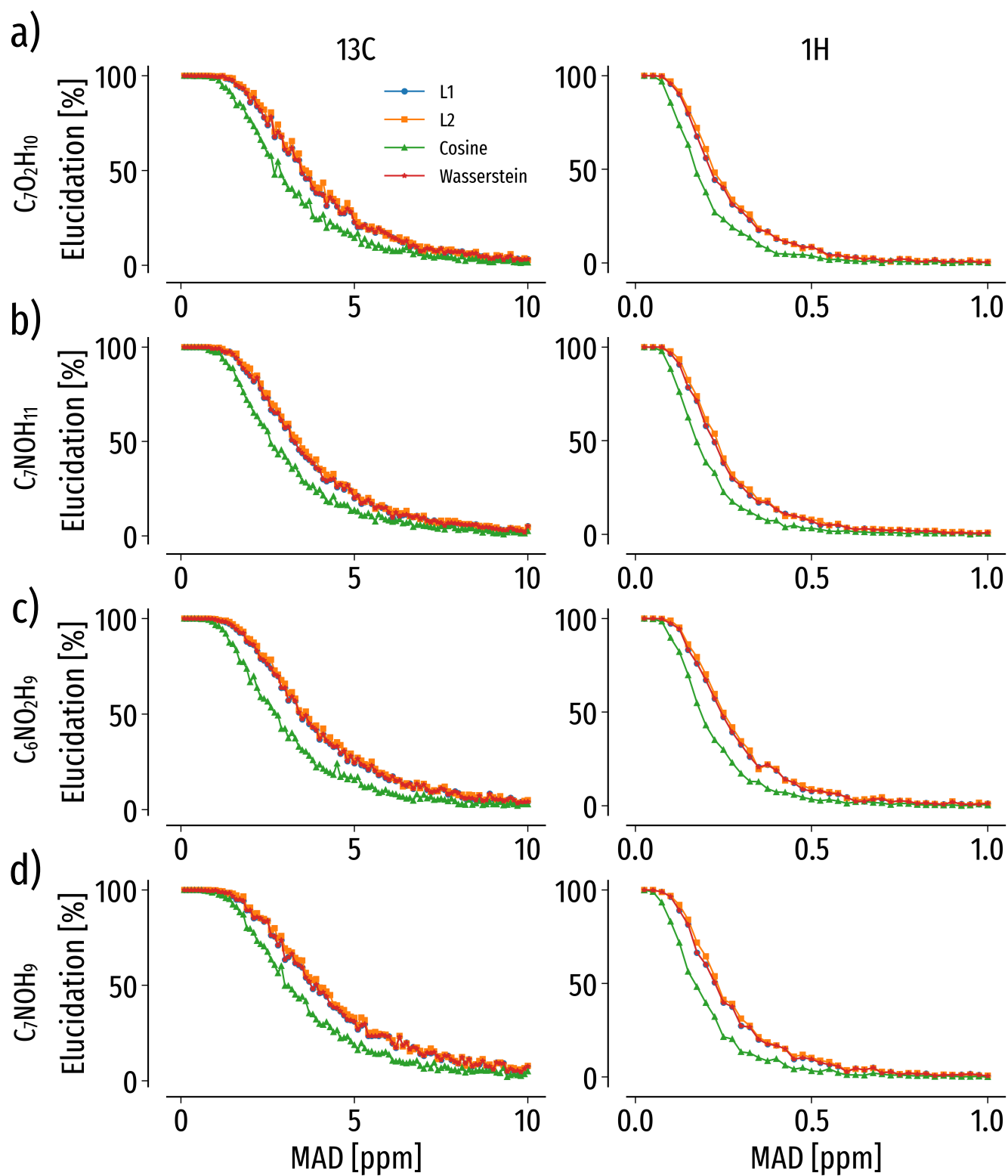


FIG. S3. Comparison of L1, L2, cosine similarity and Wasserstein distances on the ^{13}C (left) or ^1H (right) elucidation success of $\text{C}_7\text{O}_2\text{H}_{10}$ (a), $\text{C}_7\text{NOH}_{11}$ (b), $\text{C}_6\text{NO}_2\text{H}_9$ (c) and C_7NOH_9 (d) constitutional isomers.

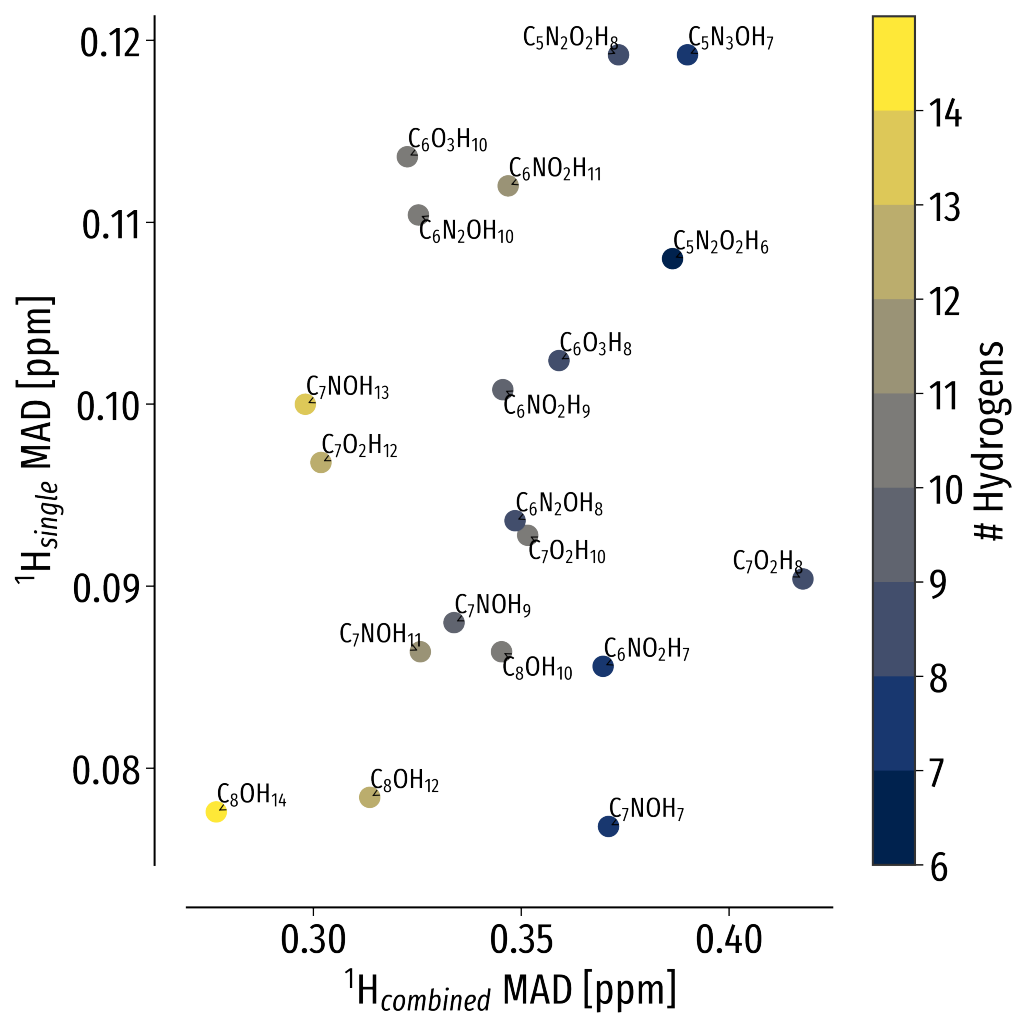


FIG. S4. Trends in QM9 chemical compound space to correctly elucidate queries at 95% accuracy. Mean absolute deviation (MAD) using only ^1H spectra ($^1\text{H}_{single}$) against ^1H and noise-free ^{13}C spectra combined ($^1\text{H}_{combined}$) at the respective N_{max} available in QM9.

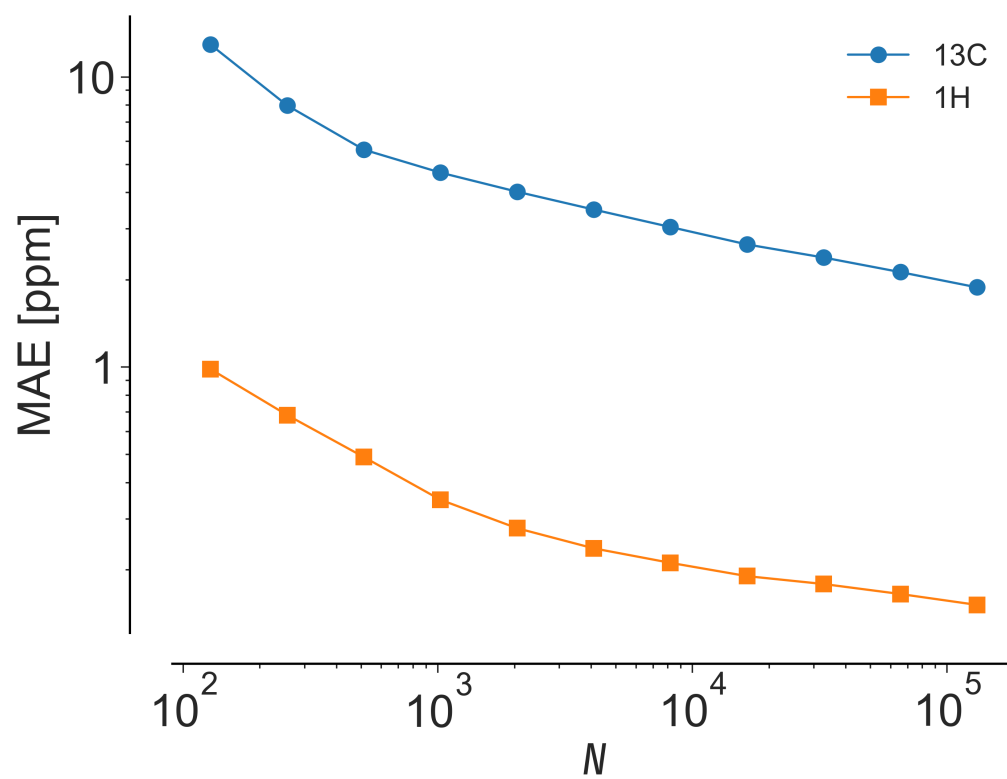


FIG. S5. Systematic improvement with increasing training set size N of KRR machine learning for ^{13}C and ^1H chemical shifts of C_8OH_{12} , C_8OH_{10} , C_8OH_{14} , $\text{C}_7\text{O}_2\text{H}_8$ and $\text{C}_7\text{O}_2\text{H}_{12}$ constitutional isomers using the FCHL19 representation.